Molecular Cell
Short Article

Intronic miR-211 Assumes the Tumor Suppressive Function of Its Host Gene in Melanoma

Carmit Levy,[1,10] Mehdi Khaled,[1,2,7,9,10] Dimitrios Iliopoulos,[5,12] Maja M. Janas,[2,7,9] Steffen Schubert,[2,7,9,11] Sophie Pinner,[2,7] Po-Hao Chen,[2,7,9] Shuqiang Li,[2,7,9] Anne L. Fletcher,[2,7] Satoru Yokoyama,[1] Kenneth L. Scott,[3] Levi A. Garraway,[3,4,9] Jun S. Song,[8] Scott R. Granter,[6] Shannon J. Turley,[2,7] David E. Fisher,[1,7,*] and Carl D. Novina[2,7,9,*]
[1]Department of Dermatology, Massachusetts General Hospital
[2]Department of Cancer Immunology and AIDS
[3]Medical Oncology
[4]Center for Cancer Genome Discovery, Dana-Farber Cancer Institute
[5]Department of Biological Chemistry and Molecular Pharmacology
[6]Pathology Department, Brigham and Women's Hospital
[7]Department of Pathology
Harvard Medical School, Boston, MA 02115, USA
[8]Institute for Human Genetics, University of California, San Francisco, San Francisco, CA 94143, USA
[9]Broad Institute of Harvard and MIT, Cambridge, MA 02141, USA
[10]These authors contributed equally to this work
[11]Present address: Cenix Bioscience, 01307 Dresden, Germany
[12]Present address: Department of Cancer Immunology and AIDS, and Department of Pathology, Harvard Medical School, Boston, MA 02115, USA
*Correspondence: dfisher3@partners.org (D.E.F.), carl_novina@dfci.harvard.edu (C.D.N.)
DOI 10.1016/j.molcel.2010.11.020

SUMMARY

When it escapes early detection, malignant melanoma becomes a highly lethal and treatment-refractory cancer. Melastatin is greatly downregulated in metastatic melanomas and is widely believed to function as a melanoma tumor suppressor. Here we report that tumor suppressive activity is not mediated by melastatin but instead by a microRNA (miR-211) hosted within an intron of melastatin. Increasing expression of miR-211 but not melastatin reduced migration and invasion of malignant and highly invasive human melanomas characterized by low levels of melastatin and miR-211. An unbiased network analysis of melanoma-expressed genes filtered for their roles in metastasis identified three central node genes: *IGF2R*, *TGFBR2*, and *NFAT5*. Expression of these genes was reduced by miR-211, and knockdown of each gene phenocopied the effects of increased miR-211 on melanoma invasiveness. These data implicate miR-211 as a suppressor of melanoma invasion whose expression is silenced or selected against via suppression of the entire melastatin locus during human melanoma progression.

INTRODUCTION

A large proportion of advanced melanomas show downregulation of melastatin, a founding member of the transient receptor potential (TRPM) cation channel family that is highly expressed in melanocytes and retinal pigmented epithelium. Whereas melastatin (*TRPM1*) is robustly expressed in benign and dysplastic nevi and in melanomas in situ, it is only variably expressed in invasive melanomas, shows widespread downregulation in melanoma metastases, and is inversely correlated with metastatic potential and prognosis of melanomas (Duncan et al., 1998, 2001). However, the mechanism(s) by which melastatin might suppress melanoma metastasis remains unknown.

Interestingly, intron 6 of the TRPM1 gene (Hunter et al., 1998) hosts the gene for miR-211, a microRNA (miRNA) whose expression is restricted to the melanocyte lineage (Gaur et al., 2007). Numerous miRNAs have been implicated in tumorigenesis (e.g., miR-17∼92 as an oncogenic cluster [He et al., 2005; O'Donnell et al., 2005]; let-7 as a tumor suppressor [Takamizawa et al., 2004; Yanaihara et al., 2006]; and miR-10b [Ma et al., 2007], miR-373 and miR-520c [Huang et al., 2008], miR-335 [Tavazoie et al., 2008], and miR-9 [Ma et al., 2010] in tumor invasion and metastasis). These observations, together with the lack of mechanistic data linking melastatin to melanoma tumor suppression, led us to hypothesize that miR-211 activity might regulate melanoma invasion and metastasis independently of its host gene function.

Melanoma short-term cultures (MSTCs) represent a physiologically relevant and an experimentally tractable cancer model because they have relatively low passage numbers since biopsy, are readily annotated with respect to genetic alterations, and are easily grown in culture. Through genetic and functional studies performed on a collection of MSTCs, we identified two populations of malignant melanomas: one with low miR-211 expression and high invasive activity, and the other with high miR-211 expression and low invasive activity. Here we report that manipulation of miR-211 levels, but not melastatin levels, alters the invasive potential of malignant melanomas, and we demonstrate a network of miR-211-responsive genes affecting melanoma invasive activity.

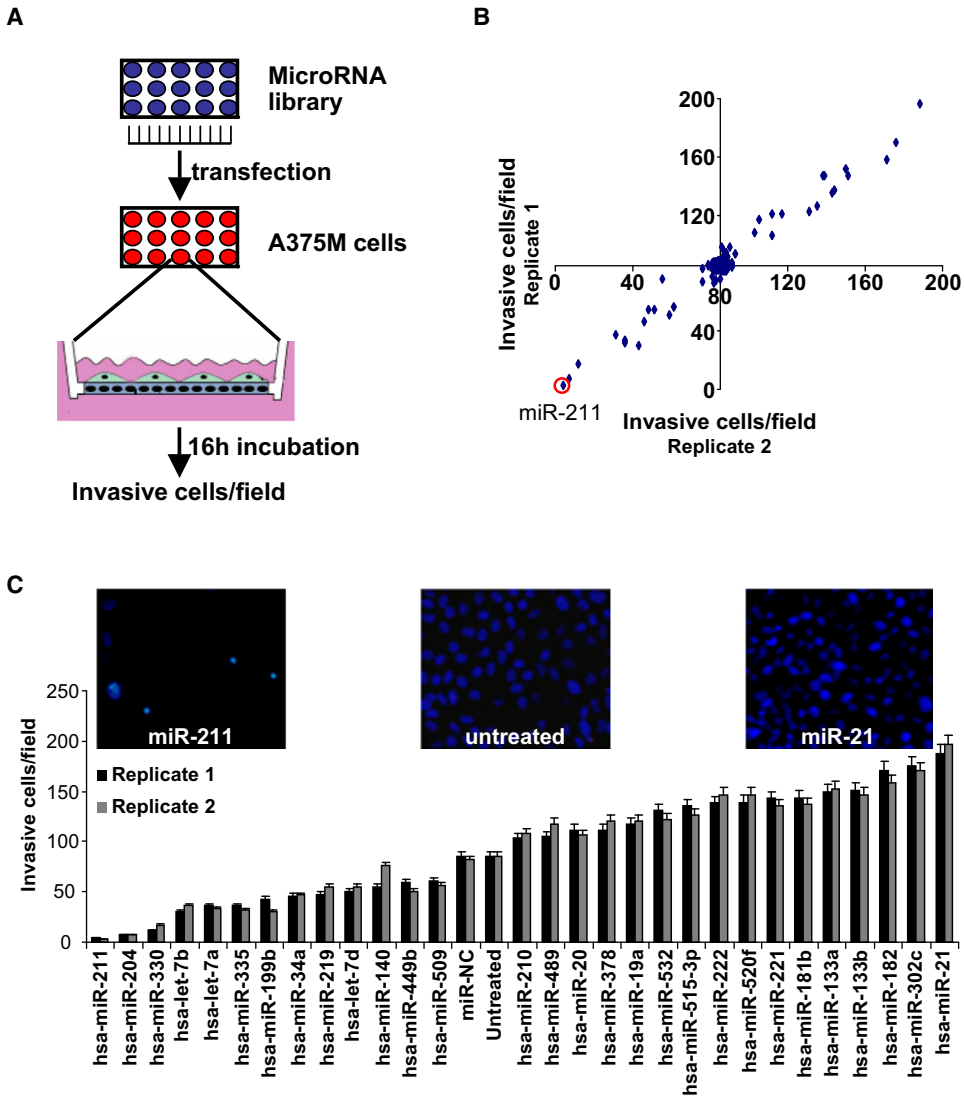

Figure 1. A Genome-wide miRNA Screen Identifies miR-211 as a Suppressor of Melanoma Invasion

(A) Screening strategy to identify miRNAs regulating A375M melanoma cell invasiveness.

(B) Number of invasive cells (average of five high-power fields) after transfection with the miRNA library in A375M cells. The experiment was performed in duplicate (replicates 1, 2).

(C) Number of invasive cells after transfection with positive hits derived from the miRNA library screen experiment. The experiment was performed in duplicate; means ± SEM.

RESULTS AND DISCUSSION

To determine whether miR-211 or other miRNAs can regulate melanoma invasiveness independently from melastatin, we performed an unbiased miRNA library screen in a highly invasive melanoma cell line, A375M (Figures 1A and 1B and see Figure S1 available online). We found that expression of the melanoma-specific miR-211 significantly decreased invasiveness of A375M cells. Interestingly, the second highest hit in this screen was the miR-211 paralog, miR-204, which is not expressed in melanocytes but shares the same seed region as miR-211 and therefore targets similar genes. Each of the miRNAs identified in the primary screen was validated and ranked by invasiveness in a secondary invasive activity screen (Figure 1C). Importantly, increased expression of tumor suppressor miRNAs miR-335 (Tavazoie et al., 2008), let-7a, let-7b, and let-7d (Takamizawa et al., 2004; Yanaihara et al., 2006) led to decreased melanoma invasiveness (Figure 1C). Conversely, increases in the oncogenic miRNAs miR-19a, miR-20 (He et al., 2005; O'Donnell et al., 2005), and miR-21 (Medina et al., 2010) led to increased melanoma invasiveness (Figure 1C).

To determine whether the expression levels of miR-211 or its host gene melastatin (Figure 2A) affect invasive activity of human melanomas, we compared mature miR-211 and its completely processed host gene mRNA levels across human melanocytes and malignant melanomas by qRT-PCR (Figure 2B).

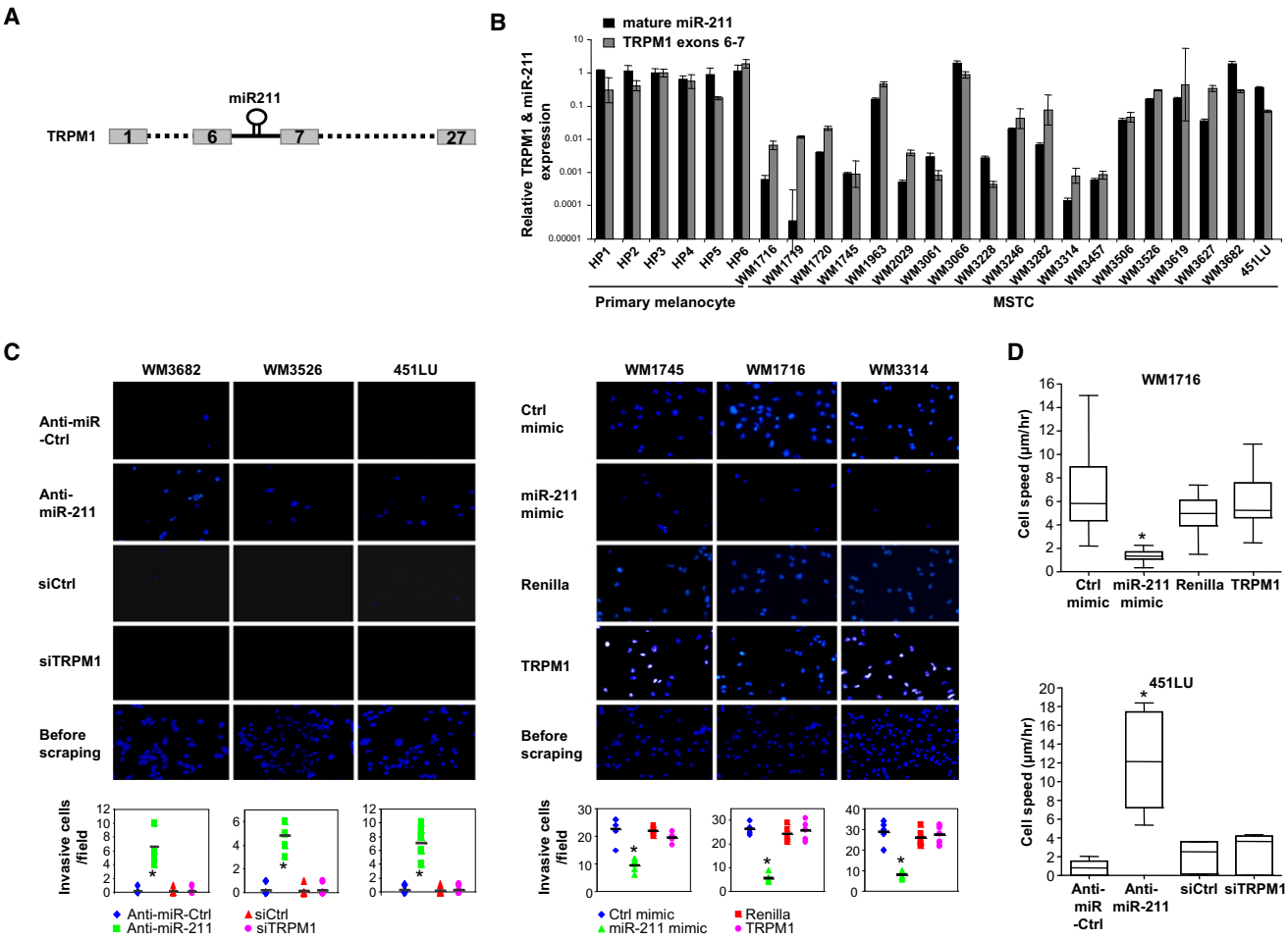

Figure 2. Perturbing miR-211 but Not Melastatin Affects Melanoma Invasion and Motility

(A) Schematic presentation of the miR-211 gene in intron 6 of the melastatin (*TRPM1*) gene.

(B) qRT-PCR of *TRPM1* (gray bars) normalized to actin, and mature miR-211 (black bars) normalized to RNU48 in multiple human primary melanocytes (HP) and melanoma short-term cultures (MSTCs). Y axis is logarithmic scale (n = 5; means ± SEM).

(C) Matrigel assays for WM3682, WM3526, and 451LU (panels at left) transfected with control antagomir (Anti-miR-Ctrl, row 1), a miR-211-specific antagomir (Anti-miR-211, row 2), a control siRNA (siCtrl, row 3), or a melastatin-specific siRNA (siTRPM1, row 4). Membranes prior to scraping noninvasive cells from the top are shown (row 5). Matrigel assays for WM1745, WM1716, or WM3314 (panels at right) transfected with control miRNA mimic (Ctrl mimic, row 1), a miR-211 mimic (miR-211-mimic, row 2), a control Renilla cDNA (Renilla), or *TRPM1* cDNA (TRPM1, row 3). The membranes prior to scraping cells from the top of the membrane are shown (row 4). Graphical presentation of the data quantifies the number of invasive cells in ten high-power fields (means ± SEM; *$p < 0.005$).

(D) Modulating miR-211 but not melastatin affects melanoma motility. Real-time video microscopy of WM1716 (top panel) expressing Renilla cDNA, melastatin cDNA (*TRPM1*), a control miRNA mimic (Ctrl mimic), or miR-211 mimic. Real-time video microscopy of 451LU (bottom panel) expressing a control antagomir (Anti-miR-Ctrl), a miR-211 antagomir (Anti-miR-211), a siRNA control (siCtrl), or a melastatin siRNA (siTRPM1). Results quantify cell migration in μm/hr (>25 representative cells analyzed for each category from two movies, means ± SEM; *$p < 0.005$). Real-time video images are added as Web-browsable links.

Consistent with possible tumor suppressor roles in melanomas, both melastatin and miR-211 were reduced in almost all malignant melanomas compared to melanocytes (Figure 2B). Linear regression analysis identified a strong direct correlation between melastatin mRNA levels and mature miR-211 levels ($R^2 = 0.73$, Figure S2A). Moreover, our data indicate that miR-211 and melastatin share a common promoter (Figures S2B–S2D), which is consistent with previous observations (Marson et al., 2008; Ozsolak et al., 2008). In addition, the expression of both genes is MITF dependent (Figures S2E–S2H). Together, these data demonstrate that the levels of melastatin and miR-211 are coordinately increased or decreased in melanomas and indicate coupled transcriptional regulation by MITF.

Next, we examined invasive activity and proliferation rates as a function of melastatin and miR-211 expression across several representative melanomas with mildly (~10-fold) and greatly (~1000-fold) reduced miR-211 levels (Figure 2B). More than 20-fold higher invasive activity was observed in melanomas with greatly reduced miR-211 levels (WM1745, WM1716, and WM3314) compared to melanomas with mildly reduced

miR-211 (WM3682, WM3526, and 451LU; Figure 2C, top panel, and Figure S2I). Consistent with reduced melastatin expression in slowly proliferating but highly invasive melanomas (Hoek et al., 2006), the doubling times of melanomas with higher melastatin and miR-211 (1.2 days and 2 days for 451LU and WM3526, respectively) were considerably shorter than the doubling times of melanomas with lower melastatin and miR-211 (more than 8 days for WM1745; Figure S2J).

To distinguish effects of miR-211 from effects of its host gene, melanomas with no reduction (WM3682) or with 10-fold reduction (WM3526 and 451LU) in melastatin and miR-211 relative to human primary melanocytes were transfected with miR-211-specific antagomirs (antisense oligonucleotides that inhibit miRNAs in a sequence-specific fashion [Krutzfeldt et al., 2005]), and the effect on melanoma invasiveness was assessed in matrigel assays (Figure 2C and Figure S2K). Inhibition of miR-211 increased melanoma invasiveness by at least 10-fold compared to a control antagomir. Importantly, knockdown of melastatin had no effect on melanoma invasiveness (Figure 2C and Figure S2K). These data indicate that melanoma invasiveness is suppressed by miR-211 but not melastatin.

The effects of increasing the expression of miR-211 were also examined. Melanomas with ~1000-fold reductions in miR-211 (WM1745, WM1716, and WM3314) relative to human primary melanocytes were transfected with a plasmid expressing a miR-211 precursor (Figure S2N). Increasing miR-211 levels in these melanomas had no effect on growth rates (Figure S2O) but reduced the invasive potential by 2- to 3-fold compared to scrambled controls (Figure 2C). In contrast, modulation of melastatin expression in these melanomas had no effect on melanoma invasiveness (Figure 2C and Figures S2L–S2N). However, increasing MITF levels reduced melanoma invasiveness, and decreasing MITF levels increased melanoma invasiveness (Figures S2G, S2H, and S2P), likely due to its effect on miR-211 expression. Modulating miR-211 had no effect on melastatin expression (Figure S2M). Similarly, modulating melastatin had no effect on miR-211 expression (Figure S2M). We conclude that changes in expression of miR-211 affect melanoma invasiveness independent of melastatin and do not affect melanoma proliferation rates.

To determine the effect of miR-211 expression levels on melanoma cell migration, we performed real-time video microscopy (Figure 2D and Supplemental Movies). WM1716 cells, expressing reduced miR-211 (Figure S2N), exhibited spindle-like morphology when cultured on a deformable collagen-matrigel matrix. When transfected with a plasmid expressing melastatin cDNA or controls (renilla luciferase cDNA or a scrambled miRNA), WM1716 demonstrated an average motility speed of approximately 5 μm/hr and maintained the spindle-like morphology. Strikingly, expression of miR-211 significantly reduced cell migration to only 1.5 μm/hr and induced rounded cell morphology. The effects of reducing miR-211 or melastatin on cell migration were also examined in 451LU cells expressing elevated miR-211. In agreement with the results in WM1716 cells, reduction of miR-211 but not melastatin increased cell motility (Figure 2D). Thus miR-211, but not melastatin, affects melanoma cell motility and invasiveness.

To discover the genetic network mediating the effects of miR-211 on melanoma invasiveness, we interrogated a literature-based set of genes restricted for melanoma expression and filtered for annotated functions in metastasis (Figure 3A and Table S1). A computationally predicted, melanoma-specific metastasis network was generated using IPA gene network software (described in the Experimental Procedures). This analysis revealed two statistically significant ($p < 10^{-5}$) gene networks, with the most statistically significant network ($p = 10^{-37}$) containing three central nodes (defined in the Experimental Procedures): *IGF2R*, *TGFBR2*, and *NFAT5* (Figure 3B and Figure S3).

To identify any function of miR-211 in the bioinformatically predicted melanoma metastasis networks, miR-211 expression data was compared to sample-matched mRNA expression data across a large collection of melanomas (Lin et al., 2008). Translational repression mediated by miRNAs is usually accompanied by reduction of target mRNA levels (Filipowicz et al., 2008). Thus, to a first approximation, potential target mRNAs are expected to demonstrate inverse correlation with miR-211. Kendall's tau (τ) rank coefficient was calculated for all mRNA/miR-211 pairs to discern concentration-dependent relationships between miR-211 and mRNAs expressed in melanomas (Figure 4A). As an internal measure of the accuracy of this analysis, a strong direct correlation was observed between the abundance of miR-211 and important target genes of MITF, including *TYRP1*, *SILV*, *MLANA*, and *CDK2* (Figure 4A) (Levy et al., 2006). A similar ranked list of genes correlated with miR-211 expression was obtained using class-dependent identification of marker genes with the ComparativeMarkerSelection module in GenePattern (data not shown). The mRNAs with significant Kendall's tau coefficients were compared with predicted targets of miR-211 using TargetScan. Confounding effects of genomic amplification were eliminated by removing mRNAs that showed increased gene copy numbers in our cell lines based on matching single nucleotide polymorphism data for those genes (Lin et al., 2008) (Table S2). Six genes were found to be represented in both the list of plausible miR-211 targets as well as the independently generated melanoma metastasis network, including *IGF2R* (TargetScan context score = −0.42), *NFAT5* (TargetScan context score = −0.06), *TGFBR2* (TargetScan context score = −0.49), *FBXW7*, *ANGPT1*, and *VHL*. Interestingly, several genes demonstrating inversely correlated expression with miR-211 levels and with lowest-rank coefficients had established roles in melanomagenesis including the central nodes *IGF2R*, *TGFBR2*, and *NFAT5*.

To determine whether these central node genes are biological targets of miR-211, the levels of miR-211 were perturbed in melanomas, and IGF2R, TGFBR2, and NFAT5 expression levels were examined (Figure 4B and Figures S4A and S4B). Reducing miR-211 in WM3526 cells increased the expression of all three mRNAs. Conversely, increasing miR-211 in WM1716 and in A375M cells reduced levels of all three mRNAs, indicating that endogenous *IGF2R*, *TGFBR2*, and *NFAT5* are biological targets of miR-211 in melanomas. To determine whether these genes are direct targets of miR-211, we transfected luciferase-expressing constructs containing the wild-type and predicted miR-211 binding site mutant 3′ untranslated regions (3′UTRs) of these

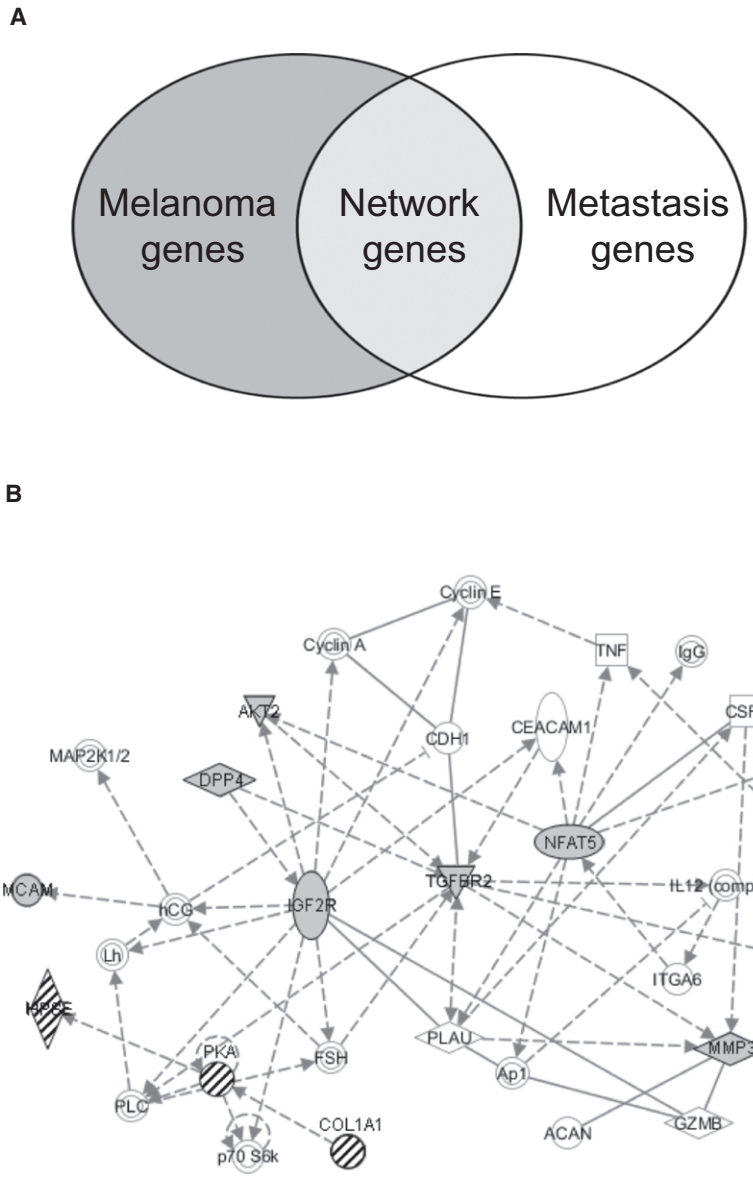

Figure 3. Gene Network Analysis Identifies Three Central Nodes Regulating Melanoma Metastasis Potentially Targeted by miR-211

(A) Literature-based melanoma and metastasis gene lists as demonstrated in the Venn diagram were used to construct the melanoma metastasis gene network.

(B) Bioinformatically predicted melanoma metastasis gene network ($p = 10^{-37}$). Solid lines indicate direct interactions, and dashed lines indicate indirect interactions. Arrows indicate activation. Lines ending in short perpendicular lines indicate repression. TargetScan-predicted miR-211 targets genes are shaded in gray (*IGFR* = −0.42, *TGFBR2* = −0.49, *NFAT* = −0.06, *DPP4* = 0.14, −0.08, AKT2 = −0.01, *MMP3* = −0.09, *ADAM19* = −0.11, −0.08, *MCAM* = −0.12). Knockdown of each central nodes gene is predicted to inhibit the entire metastasis network except for the genes indicated by hatch marks.

genes into HeLa cells (which lack endogenous miR-211) with or without a miR-211 mimic. Unexpectedly, *TGFBR2* and *NFAT5*, but not *IGF2R*, were shown to be direct targets of miR-211 (Figure 4C).

Because miR-211 affects endogenous expression of the central node genes, we tested the effect of knockdown of these genes on melanoma invasive activity. Interestingly, knockdown of any central node gene phenocopied the effect of increasing miR-211 levels in melanomas with high levels of *IGF2R*, *TGFBR2*, and *NFAT5* (Figure 4D). Consistent with a lack of direct interaction between these genes as predicted bioinformatically (Figure 3B), knockdown of each central node gene did not affect the expression of the other central node genes (Figure S4C). However, we noted that one direct input to *IGF2R* is *DPP4*, which has two predicted miR-211 binding sites (TargetScan context score = 0.14 and −0.08). Knockdown of the peripheral node gene *DPP4*, but not *ADAM19* (another predicted miR-211 target gene), phenocopied the effect of increased miR-211 on melanoma invasiveness (Figure 4D and Figures S4D and S4E). Interestingly, knockdown of *DPP4* also led to reduced expression of *IGF2R*, *TGFBR2*, and *NFAT5* (Figure S4D). These data demonstrate the high-predictive index of the melanoma metastasis network and provide a mechanistic basis for reduced IGF2R expression upon increased miR-211 expression. Together, our data indicate that increasing miR-211 directly represses *NFAT5* and *TGFBR2*, and indirectly represses *IGF2R*, leading to the reduction of the invasive potential of malignant melanomas.

Here we report an intronic miRNA that assumes a tumor suppressive function previously ascribed to its host gene. Reducing miR-211 but not melastatin levels is sufficient to convert a noninvasive melanoma to an invasive melanoma. Conversely, increasing miR-211 but not melastatin is sufficient to convert an invasive melanoma to a noninvasive melanoma. Previous observations comparing primary melanomas identified reduced expression of melastatin in distant metastasis (Duncan et al., 1998, 2001) and an inverse correlation between melastatin expression and tumor thickness (Deeds et al., 2000). Our data raise the possibility, however, that these observations may have been due to altered expression levels of miR-211. Because miRNA genes are frequently hosted by protein-coding genes, phenotypes attributed to genetic deletion of protein-coding genes may actually be attributable to abrogated expression of the hosted miRNAs (Moffett and Novina, 2007).

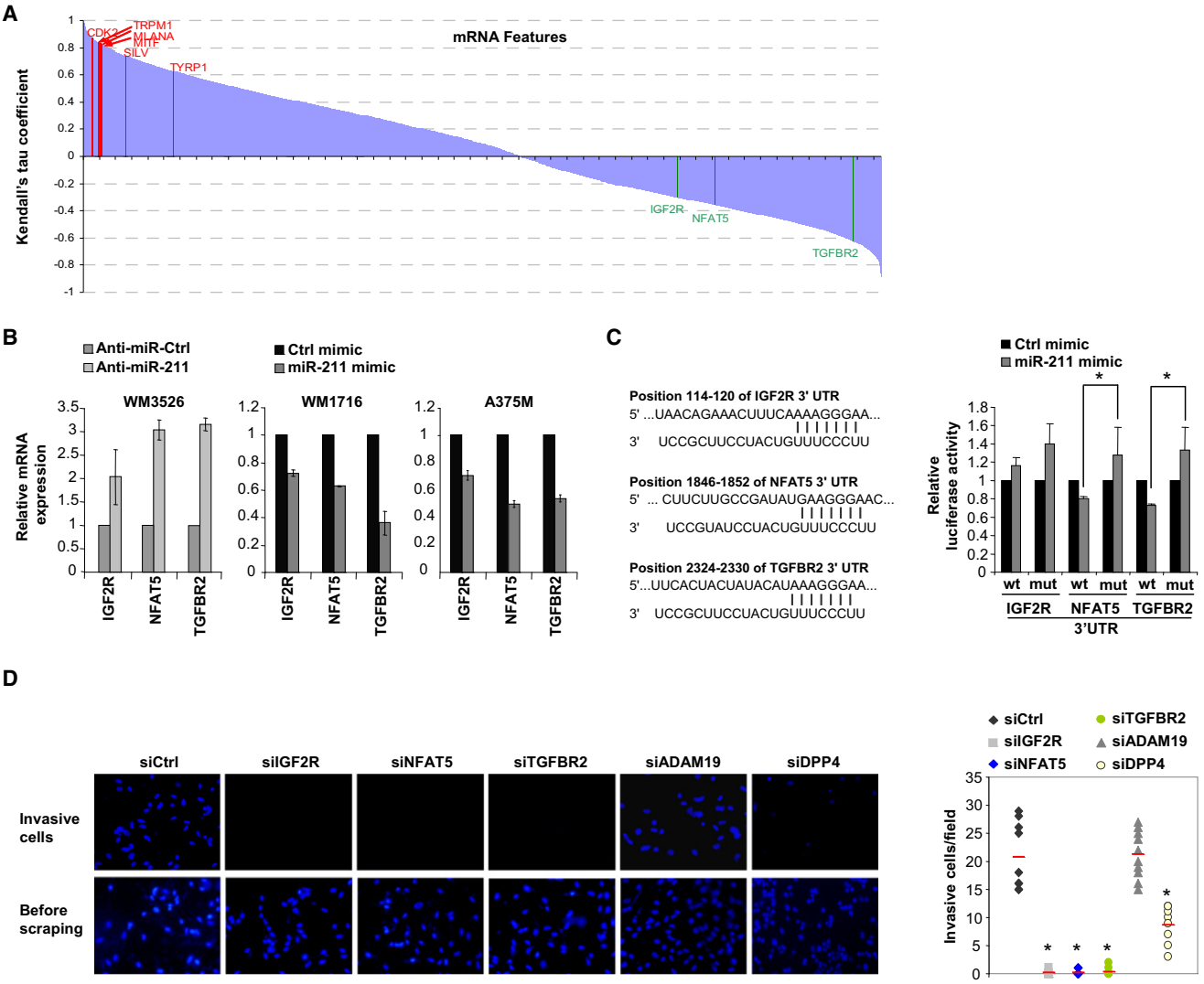

Figure 4. miR-211 Targets Multiple Genes Regulating Melanoma Metastasis

(A) Statistical association analysis of previously published mRNA profiling data (13,211 transcripts) versus miR-211 expression using Kendall's tau. mRNA names are sorted by Kendall's tau coefficient and periodically listed on the horizontal axis. Magnitude of coefficient measures the degree of association, and a negative coefficient denotes an inverse association. Representative melanoma-relevant genes directly correlated with miR-211 are highlighted in red: *MLANA* ($\tau = 0.831$), *MITF* ($\tau = 0.821$), *CDK2* ($\tau = 0.776$), *SILV* ($\tau = 0.738$), and *TYRP1* ($\tau = 0.627$). Predicted miR-211 target genes are inversely correlated with miR-211 and are highlighted in green: *IGF2R* ($\tau = -0.297$), *NFAT5* ($\tau = -0.357$), and *TGFB2R* ($\tau = -0.620$).

(B) miR-211 represses endogenous *IGF2R*, *NFAT*, and *TGFBR2* expression in melanoma cells. Transfection of a miR-211 antagomir into WM3526 derepresses *IGF2R*, *NFAT5*, and *TGFBR2* expression compared to a control antagomir (Anti-miR-Ctrl). Transfection of a miR-211 mimic into WM1716 or A375M represses *IGF2R*, *NFAT5*, and *TGFBR2* expression compared to a control miRNA mimic (Ctrl mimic). n = 3; means ± SEM.

(C) *NFAT5* and *TGFBR2* but not *IGF2R* are direct miR-211 target genes. Schematic presentation of predicted miR-211 target sites identified in the *IGF2R*, *NFAT5*, or *TGFBR2*. Numbers indicate positions of miR-211 binding sites on target mRNA 3′UTRs. HeLa cells were transfected with luciferase constructs possessing wild-type (WT) or miR-211 binding site mutant (mut) 3′UTRs of *IGF2R*, *NFAT5*, or *TGFBR2* and with a miR-211 mimic or a control miRNA mimic (Ctrl Mimic). n = 5; means ± SEM.

(D) Knockdown of *IGF2R*, *NFAT5*, or *TGFBR2* phenocopies the effect of increasing miR-211 on melanoma invasive activity. WM1716 cells were transfected with a control siRNA (siCtrl), or siRNAs against indicated genes and subjected to matrigel assays. Invasive cells were counted (top panels) and are quantitated (graphs, right). The bottom panels demonstrate the membranes prior to scraping (n = 3; means ± SEM).

TGFB has been implicated in the metastatic spread of melanoma and other cancers (Giampieri et al., 2009; Pinner et al., 2009; Van Belle et al., 1996). TGFB signaling has also been shown to promote hypopigmentation (Martinez-Esparza et al., 1997; Pinner et al., 2009), downregulation of MITF (which controls the melastatin/miR-211 locus [Miller et al., 2004]), disruption of cell-cell adhesion, single-cell invasion to escape the primary tumor, and invasion of blood vessels (Giampieri

et al., 2009). Therefore, increased TGFB signaling through increased TGFBR2 expression might partially explain increased melanoma invasion and motility when miR-211 levels are low. To our knowledge, *NFAT5* and *IGF2R* have not been previously linked to melanoma metastasis. Several other genes represented in the melanoma metastasis network are predicted targets of miR-211 and demonstrate reduced expression upon increased miR-211 (Figure 4 and data not shown). These genes may participate in miR-211-regulated melanoma invasion or subsequent steps of melanoma metastasis.

Complex phenotypes such as changes in cell morphology, motility, and invasiveness are rarely regulated by a single gene. Because a single miRNA may target thousands of genes, it is possible that altered expression of a single miRNA can regulate complex phenotypes. It has been suggested that therapeutic manipulation of a single miRNA may result in the regulation of many genes and may affect the "normalization" of a disease phenotype (Wurdinger and Costa, 2007). Our data suggest that modulating miR-211 or its target gene levels may pave the way toward new therapies for metastatic melanoma.

EXPERIMENTAL PROCEDURES

Cell Culture

HeLa cells and A375M cells were cultured in DMEM medium supplemented with 10% FBS and 1% penicillin-streptomycin.

MSTCs were selected from cryopreserved collections at the Wistar Institute (62 lines), the University Hospital of Zurich (24 lines), and the Dana-Farber Cancer Institute (DFCI, 37 lines). All MSTCs were cultured in RPMI medium (MediaTech) supplemented with 10% fetal bovine serum (MediaTech) and 1% penicillin/streptomycin/glutamine (Invitrogen), except for DFCI MSTCs, which were cultivated in DMEM (MediaTech) supplemented with 10% serum. For some Wistar lines, to enhance cell adherence, tissue culture dishes were first coated with 1% porcine gel solution (Sigma). Primary human melanocytes were isolated and grown from neotal foreskins as described (McGill et al., 2002). Primary melanocytes between passages 2 and 5 were stimulated with 20 uM forskolin (Sigma Aldrich) for indicated times after an overnight starvation in F10 medium supplemented only with penicillin/streptomycin/glutamine. For microarrays, primary melanocytes were stimulated for 16 hr with forskolin. 501mel human melanoma cells (gift from Dr. Ruth Halaban, Yale University) were maintained in Ham's F-10 media (Mediatech) supplemented with 10% fetal bovine serum (FBS, Sigma Aldrich) and 1% penicillin/streptomycin/glutamine (PSQ). UACC62 human melanoma cell line was obtained from NCI and maintained in RPMI-1640 media (Mediatech) supplemented with 10% fetal bovine serum (FBS) (Sigma Aldrich) and 1% penicillin/streptomycin/glutamine (PSQ).

Genome-wide miRNA Screen

A miRNA library of 300 precursor miRNAs (Ambion, Inc.) was transfected in triplicate (100 nM) using siPORT *NeoFX* into A375M cells, seeded in 24-well plates. SiPORT *NeoFX* is a lipid transfection agent consisting of a mixture of lipids that spontaneously complex small interfering RNAs and facilitates its transfer to the cells. After 24 hr, cells were serum starved overnight. 1×10^5 cells were added to invasion chambers coated with Matrigel (BD Biosciences), and cells were allowed to invade for 16 hr toward media containing 10% FBS. Cells remaining on the top side of the membrane were removed using a cotton swab, and invading cells were counted in five fields per insert. The library experiment was performed in duplicate. No cell toxicity from the transfection agent was detected. Transfection conditions were optimized with a miRNA negative control (AM17110, Ambion, Inc.) and miR-182 as a positive control. For validation, the 29 precursor miRNAs identified from the primary screen were transfected into A375M cells and seeded in 24-well plates, and the invasion assay was repeated. Each miRNA was transfected in triplicate.

RNA Purification and qRT-PCR

Total RNA was purified using TRIzol reagent (Invitrogen) according to the manufacturer's instructions, followed by treatment with RNase-free DNase (QIAGEN). Dried RNA pellets were resuspended in appropriate volumes of DEPC/ddH_2O. RNA was quantified by measuring $OD_{260/280}$. For qRT-PCR analysis of mature miR-211 or miR-107, 10 ng total RNA was used in a TaqMan miRNA assay according to the manufacturer's protocols (Applied Biosystems). Mature miR-211 expression was normalized to expression of RNU48, also detected by TaqMan assay (Applied Biosystems). For qRT-PCR analysis of *TRPM1*, *NFAT5*, *IGF2R*, *TGFBR2*, and other genes, RNA was subjected to one-step qRT-PCR using a QuantiTect RT-PCR kit (QIAGEN) and iQ SYBRgreen Supermix (Bio-Rad). Primer sequences and manufacturers are listed in Table S3. All experiments are $n \geq 3$. Standard error of the mean (SEM) is presented.

Oligonucleotide Transfection

MiRNA mimics, antagomirs, or siRNAs were transfected into MSTCs using HiPerFect according to the manufacturer's protocols (QIAGEN). The sequences and manufacturers of the miR-211 mimic, miR-211 antagomir, control miRNA mimic, control antagomir, *TRPM1*, *NFAT5*, *IGF2R*, *TGFBR2*, *DPP4* and *ADAM19* siRNA, and control siRNA are listed in Table S4. Cells were transfected twice with 100 pmol of oligonucleotide per well (0.5×10^6 cells) at 24 hr intervals. Transfected MSTCs were assayed 48 hr after the second transfection.

Invasion and Migration Assays

MSTCs were transfected with oligonucleotides as described above. Forty-eight hours after the second transfection, cells were serum starved overnight. Fifty thousand cells were added in duplicate to invasion chambers coated with Matrigel (BD Biosciences). Cells were allowed to invade for 9 hr toward media containing 10% FBS. Cells remaining on the top side of the membrane were removed using a cotton swab, and invading cells were fixed and stained with 4′-6-diamidino-2-phenylindole (DAPI, Vector Laboratories Inc.). In all assays, ten fields per insert were photographed, and scored SEM was measured.

Cell Growth and Metabolic Rate Assay

Cells (10^4/well) were plated in multiple 24-well plates. The following day was considered day 0. For analysis of cell growth/number, cells were fixed using 10% ethanol/10% acetic acid and stained with 0.2% crystal violet fixative. Following washes with water, the plates were dried. Each 24-well plate was quantified by crystal violet staining. The crystal violet dye was redissolved in fixation solution. One hundred microliters of the redissolved dye was used for color measurement, in duplicate. Color intensity was measured at OD_{595} in a 96-well plate reader and normalized to day 0 as 100%. For metabolic rate tests, 5×10^4 cells were cultured in 96-well plates, and cell proliferation assays were performed 48 hr after siRNA, miRNA, or control nucleic acid transfection. The cell proliferation reagent WST-1 (Roche) was added and cell proliferation was measured according to the manufacturer's instructions (Roche). All experiments are $n \geq 3$, and SEM is presented.

Microscopy Real-Time Cell Mobility

A ZeissLSM510META confocal microscope was used. Analysis of cell migration speed was performed as described (Pinner et al., 2009) by tracking phase-contrast movies of primary melanoma cell lines plated on collagen-matrigel gels (Hooper et al., 2006) spread on 24-well glass-bottomed plates (MatTek corporation). Multiposition imaging was conducted over 10 hr, and images were acquired at 10 min intervals. Mobility of Cherry/GFP-positive cells (>25 cells) was measured from each movie. Tracks were calculated using ImageJ and Excel software.

Gene Network Analysis

Gene networks were constructed and identified important hubs using Ingenuity Gene Network Analysis. Specifically, we created a melanoma-metastasis gene list including common genes derived from a literature-based melanoma gene list and a literature-based metastasis gene list. These literature-based gene lists were created using IPA software analysis (Ingenuity,

Inc.). Using this melanoma metastasis gene list, we performed gene network analysis. Pathways of highly interconnected genes were identified by statistical likelihood using the equation

$$\text{Score} = -\log_{10}\left(1 - \sum_{i=0}^{f-1} \frac{C(G,i)C(N-G,s-i)}{C(N,s)}\right)$$

where N is the number of genes in the network of which G are central node genes, for a pathway of s genes of which f are central node genes. C(n,k) is the binomial coefficient. Central nodes are considered genes with very high flux capacity (total number of incoming and outgoing links higher than 9). The flux capacity score for *TGFBR2* is 10, for *NFAT5* is 9, and for *IGF2R* is 12. The nodes with flux capacity score lower than 9 were considered peripheral nodes. We considered statistically significant gene networks those with a p value $< 10^{-10}$. Gray color indicates genes included in the melanoma-metastasis gene list. Solid lines indicate direct gene interactions, while dashed lines indicate indirect gene interactions.

Hierarchical Clustering of Genomic Profiles

An input matrix was generated by calculating the base-2 logorithm of normalized mRNA expression profiles. The input matrix was visualized in TIGR MeV v4.1 (http://www.tm4.org/mev.html). Both the gene tree and the sample tree were generated using Euclidean distance and average linkage.

Unsupervised Rank Correlation of Microarrays

To identify concentration-dependent relationships involving miR-211, rigid nonparametric association statistical analyses were performed. Computations were done using scripts written in Python (http://www.python.org/) and the SciPy module (http://www.scipy.org/). A matrix was generated with each column of the input representing mRNA expression values from a single culture and each row of the input representing expression values for each gene. A copy of the miR-211 expression array was then paired with each row of the input matrix, and the association between each pair was evaluated by calculating the Kendall's tau rank coefficient.

Class-Dependent Identification of Marker Genes

MSTCs were separated into three classes based on miR-211 expression level: high, medium, and low. Only the "high" and "low" classes are used in the actual calculation. For each gene, the degree of difference in mRNA expression between the "high" and "low" classes were measured using pairwise, two-sided t test and median values in each class. The calculations were done with 1000 iterations and smooth p values through the ComparativeMarkerSelection module in the GenePattern software suite (http://genepattern.broad.mit.edu/; version 3.1.1). Genes were ranked by t test score. A negative score denotes an inverse relationship between a gene's mRNA expression and miR-211 expression, whereas a positive score denotes a direct relationship.

Combination Analysis of Correlation with miRNA and Target Prediction

Computationally predicted mRNA targets for *Homo sapiens* miR-211 (hsa-miR-211) were identified using a database from Memorial Sloan-Kettering Cancer Center (http://www.microrna.org/) as the first input for this analysis. The second input comprised a list of genes whose differential mRNA expressions had strong negative correlation with miR-211 expression from unsupervised rank correlation analysis. The two inputs were combined to identify overlaps.

Plasmid Construction and Stable Cell Line Establishment

PLKO.1 vector was modified by replacing the puromycin resistance cassette with a cassette coding for luciferase, mCherry, and puromycin using BamHI and KpnI restriction sites. This vector was used for miRNA overexpression. For cDNA overexpression, the U6 promoter of the vector described above was replaced by a HPGK promoter using SanDI and AgeI.

For establishement of stable cell lines, MSTCs were seeded in a 6-well dish and transfected the modified PLKO.1 vectors using FugeneHD (Roche). After 2 days, the cells were grown with 1 μg/ml puromicyn. After 4–6 weeks, the cells were used for experiments.

SUPPLEMENTAL INFORMATION

Supplemental Information includes Supplemental Experimental Procedures, four figures, four tables, six movies, and Supplemental References and can be found with this article online at doi:10.1016/j.molcel.2010.11.020.

ACKNOWLEDGMENTS

We would like to gratefully acknowledge Dr. Meenhard Herlyn for supplying several melanoma short-term cultures for these studies. We also wish to thank Dr. Andrew Kung and Dr. Hans Wildund for insightful discussions. This work was funded by National Institutes of Health (NIH) grant AR043369 (D.E.F.), the Melanoma Research Alliance (D.E.F), the Adelson Medical Research Foundation (D.E.F.), The US-Israel Binational Science Foundation (D.E.F.), the Doris Duke Medical Foundation (D.E.F.), the Doris Duke Medical Foundation (C.D.N.), and by American Cancer Society (C.D.N.). S.L. was supported by NRSA Fellowship (NIH/NCI T32 CA070083).

Received: July 20, 2010
Revised: September 27, 2010
Accepted: October 21, 2010
Published online: November 24, 2010

REFERENCES

Deeds, J., Cronin, F., and Duncan, L.M. (2000). Patterns of melastatin mRNA expression in melanocytic tumors. Hum. Pathol. *31*, 1346–1356.

Duncan, L.M., Deeds, J., Hunter, J., Shao, J., Holmgren, L.M., Woolf, E.A., Tepper, R.I., and Shyjan, A.W. (1998). Down-regulation of the novel gene melastatin correlates with potential for melanoma metastasis. Cancer Res. *58*, 1515–1520.

Duncan, L.M., Deeds, J., Cronin, F.E., Donovan, M., Sober, A.J., Kauffman, M., and McCarthy, J.J. (2001). Melastatin expression and prognosis in cutaneous malignant melanoma. J. Clin. Oncol. *19*, 568–576.

Filipowicz, W., Bhattacharyya, S.N., and Sonenberg, N. (2008). Mechanisms of post-transcriptional regulation by microRNAs: are the answers in sight? Nat. Rev. Genet. *9*, 102–114.

Gaur, A., Jewell, D.A., Liang, Y., Ridzon, D., Moore, J.H., Chen, C., Ambros, V.R., and Israel, M.A. (2007). Characterization of microRNA expression levels and their biological correlates in human cancer cell lines. Cancer Res. *67*, 2456–2468.

Giampieri, S., Manning, C., Hooper, S., Jones, L., Hill, C.S., and Sahai, E. (2009). Localized and reversible TGFbeta signalling switches breast cancer cells from cohesive to single cell motility. Nat. Cell Biol. *11*, 1287–1296.

He, L., Thomson, J.M., Hemann, M.T., Hernando-Monge, E., Mu, D., Goodson, S., Powers, S., Cordon-Cardo, C., Lowe, S.W., Hannon, G.J., and Hammond, S.M. (2005). A microRNA polycistron as a potential human oncogene. Nature *435*, 828–833.

Hoek, K.S., Schlegel, N.C., Brafford, P., Sucker, A., Ugurel, S., Kumar, R., Weber, B.L., Nathanson, K.L., Phillips, D.J., Herlyn, M., et al. (2006). Metastatic potential of melanomas defined by specific gene expression profiles with no BRAF signature. Pigment Cell Res. *19*, 290–302.

Hooper, S., Marshall, J.F., and Sahai, E. (2006). Tumor cell migration in three dimensions. Methods Enzymol. *406*, 625–643.

Huang, Q., Gumireddy, K., Schrier, M., le Sage, C., Nagel, R., Nair, S., Egan, D.A., Li, A., Huang, G., Klein-Szanto, A.J., et al. (2008). The microRNAs miR-373 and miR-520c promote tumour invasion and metastasis. Nat. Cell Biol. *10*, 202–210.

Hunter, J.J., Shao, J., Smutko, J.S., Dussault, B.J., Nagle, D.L., Woolf, E.A., Holmgren, L.M., Moore, K.J., and Shyjan, A.W. (1998). Chromosomal

localization and genomic characterization of the mouse melastatin gene (Mlsn1). Genomics *54*, 116–123.

Krutzfeldt, J., Rajewsky, N., Braich, R., Rajeev, K.G., Tuschl, T., Manoharan, M., and Stoffel, M. (2005). Silencing of microRNAs in vivo with 'antagomirs'. Nature *438*, 685–689.

Levy, C., Khaled, M., and Fisher, D.E. (2006). MITF: master regulator of melanocyte development and melanoma oncogene. Trends Mol. Med. *12*, 406–414.

Lin, W.M., Baker, A.C., Beroukhim, R., Winckler, W., Feng, W., Marmion, J.M., Laine, E., Greulich, H., Tseng, H., Gates, C., et al. (2008). Modeling genomic diversity and tumor dependency in malignant melanoma. Cancer Res. *68*, 664–673.

Ma, L., Teruya-Feldstein, J., and Weinberg, R.A. (2007). Tumour invasion and metastasis initiated by microRNA-10b in breast cancer. Nature *449*, 682–688.

Ma, L., Young, J., Prabhala, H., Pan, E., Mestdagh, P., Muth, D., Teruya-Feldstein, J., Reinhardt, F., Onder, T.T., Valastyan, S., et al. (2010). miR-9, a MYC/MYCN-activated microRNA, regulates E-cadherin and cancer metastasis. Nat. Cell Biol. *12*, 247–256.

Marson, A., Levine, S.S., Cole, M.F., Frampton, G.M., Brambrink, T., Johnstone, S., Guenther, M.G., Johnston, W.K., Wernig, M., Newman, J., et al. (2008). Connecting microRNA genes to the core transcriptional regulatory circuitry of embryonic stem cells. Cell *134*, 521–533.

Martinez-Esparza, M., Jimenez-Cervantes, C., Beermann, F., Aparicio, P., Lozano, J.A., and Garcia-Borron, J.C. (1997). Transforming growth factor-beta1 inhibits basal melanogenesis in B16/F10 mouse melanoma cells by increasing the rate of degradation of tyrosinase and tyrosinase-related protein-1. J. Biol. Chem. *272*, 3967–3972.

McGill, G.G., Horstmann, M., Widlund, H.R., Du, J., Motyckova, G., Nishimura, E.K., Lin, Y.L., Ramaswamy, S., Avery, W., Ding, H.F., et al. (2002). Bcl2 regulation by the melanocyte master regulator Mitf modulates lineage survival and melanoma cell viability. Cell *109*, 707–718.

Medina, P.P., Nolde, M., and Slack, F.J. (2010). OncomiR addiction in an in vivo model of microRNA-21-induced pre-B-cell lymphoma. Nature *467*, 86–90.

Miller, A.J., Du, J., Rowan, S., Hershey, C.L., Widlund, H.R., and Fisher, D.E. (2004). Transcriptional regulation of the melanoma prognostic marker melastatin (TRPM1) by MITF in melanocytes and melanoma. Cancer Res. *64*, 509–516.

Moffett, H.F., and Novina, C.D. (2007). A small RNA makes a Bic difference. Genome Biol. *8*, 221.

O'Donnell, K.A., Wentzel, E.A., Zeller, K.I., Dang, C.V., and Mendell, J.T. (2005). c-Myc-regulated microRNAs modulate E2F1 expression. Nature *435*, 839–843.

Ozsolak, F., Poling, L.L., Wang, Z., Liu, H., Liu, X.S., Roeder, R.G., Zhang, X., Song, J.S., and Fisher, D.E. (2008). Chromatin structure analyses identify miRNA promoters. Genes Dev. *22*, 3172–3183.

Pinner, S., Jordan, P., Sharrock, K., Bazley, L., Collinson, L., Marais, R., Bonvin, E., Goding, C., and Sahai, E. (2009). Intravital imaging reveals transient changes in pigment production and Brn2 expression during metastatic melanoma dissemination. Cancer Res. *69*, 7969–7977.

Takamizawa, J., Konishi, H., Yanagisawa, K., Tomida, S., Osada, H., Endoh, H., Harano, T., Yatabe, Y., Nagino, M., Nimura, Y., et al. (2004). Reduced expression of the let-7 microRNAs in human lung cancers in association with shortened postoperative survival. Cancer Res. *64*, 3753–3756.

Tavazoie, S.F., Alarcon, C., Oskarsson, T., Padua, D., Wang, Q., Bos, P.D., Gerald, W.L., and Massague, J. (2008). Endogenous human microRNAs that suppress breast cancer metastasis. Nature *451*, 147–152.

Van Belle, P., Rodeck, U., Nuamah, I., Halpern, A.C., and Elder, D.E. (1996). Melanoma-associated expression of transforming growth factor-beta isoforms. Am. J. Pathol. *148*, 1887–1894.

Wurdinger, T., and Costa, F.F. (2007). Molecular therapy in the microRNA era. Pharmacogenomics J. *7*, 297–304.

Yanaihara, N., Caplen, N., Bowman, E., Seike, M., Kumamoto, K., Yi, M., Stephens, R.M., Okamoto, A., Yokota, J., Tanaka, T., et al. (2006). Unique microRNA molecular profiles in lung cancer diagnosis and prognosis. Cancer Cell *9*, 189–198.